

Supplementary Information

An on-demand nanofluidic concentrator

Miao Yu,^a Youmin Hou,^b Hongbo Zhou,^{b,c} and Shuhuai Yao^{*a,b}

^a Bioengineering Graduate Program, Biomedical Engineering Division, The Hong Kong University of Science and Technology, Hong Kong, China.

^b Department of Mechanical and Aerospace Engineering, The Hong Kong University of Science and Technology, Hong Kong, China.

^c State Key Laboratory of Transducer Technology, Shanghai Institute of Microsystem and Information Technology, Chinese Academy of Sciences, China.

S1. Fabrication and alignment of the nanochannel array

An array of nanochannels were fabricated on a PS Petri dish lid, within a 1 cm × 1 cm area defined by a thin PDMS frame (Fig. S1(a)). The PDMS frame was firstly reversibly bonded to the PS surface after 30 s O₂ plasma treatment. The petri dish containing 3 mL ethanol was placed on a hot plate at 80 °C for 10 hours, resulting in a uniformly distributed array of nanoslits on the PS surface. The PDMS frame was removed after the fabrication. To align the nanoslits with the microchannels in the PDMS replica, we used a home-made alignment system coupled with a microscope. The number of the effective nanoslits can be varied by changing the length of the microchannels. Fig. S1(b) shows a device in which eight nanochannels are integrated with the microchannels.

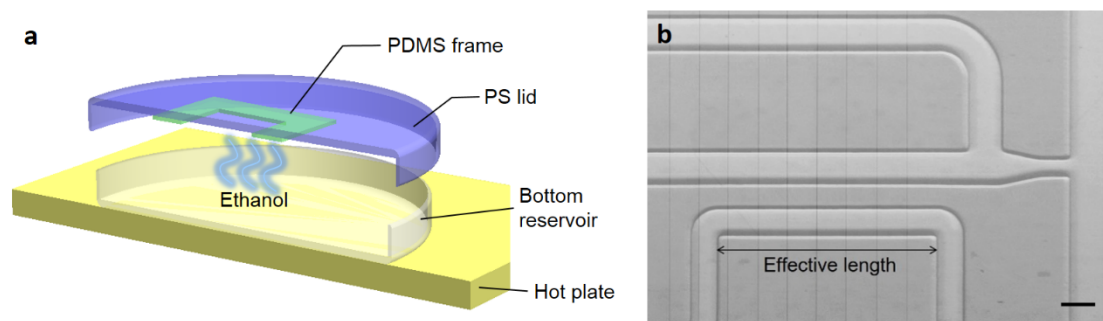


Figure S1. (a) Setup for fabricating the nanochannel array in a PDMS-frame defined area on a PS Petri dish. (b) Optical image of the chip (scale bar 50 μm).

S2. Experimental setup

A schematic of the proposed system is shown in Fig. S2. The external pressure P_c is varied by adjusting the height of the syringe connected to the reservoirs of the control channel. The external pressure can be calculated as $P_c = \rho g \Delta h$, where ρ is the density of solution, g is gravity acceleration, and Δh is the height difference of the reservoirs between the control and concentration channels.

S3. Intensity calibration

During the ICP process, the concentration of the sample molecules may vary several orders of magnitude. Since the dynamic range of a CCD is limited, simultaneous detection of both the diluted and concentrated sample intensities is often not possible using the same imaging process. The signal of the diluted sample may be below the limit of detection, while that of an enriched sample may saturate the CCD. To properly determine the preconcentration factor for our experiments, we carried out a calibration for the raw intensity

data obtained from experiments. First, the raw intensity I_{raw} was subtracted by the background intensity I_{bg} . As illustrated by Fig. S3(a), The corrected intensity is defined as $I_{\text{corr}} = I_{\text{raw}} - I_{\text{bg}}$. Then, the channel was filled with a series of sample solutions at known concentrations. For each concentration, the background subtracted intensity was obtained by averaging within a droplet. To accommodate the drastic changes in signals, we adjusted the exposure time of the CCD. As shown by the results of the calibration experiment in Fig. S3(b), the background-subtracted intensity is linearly proportional to the exposure time, Δt . Therefore, the data collected using different exposure times can be normalized as $I_{\text{norm}} = I_{\text{corr}} / \Delta t$. The calibration curve for FITC-BSA is shown in Fig. S3(c), which can be used to determine the preconcentration factor.

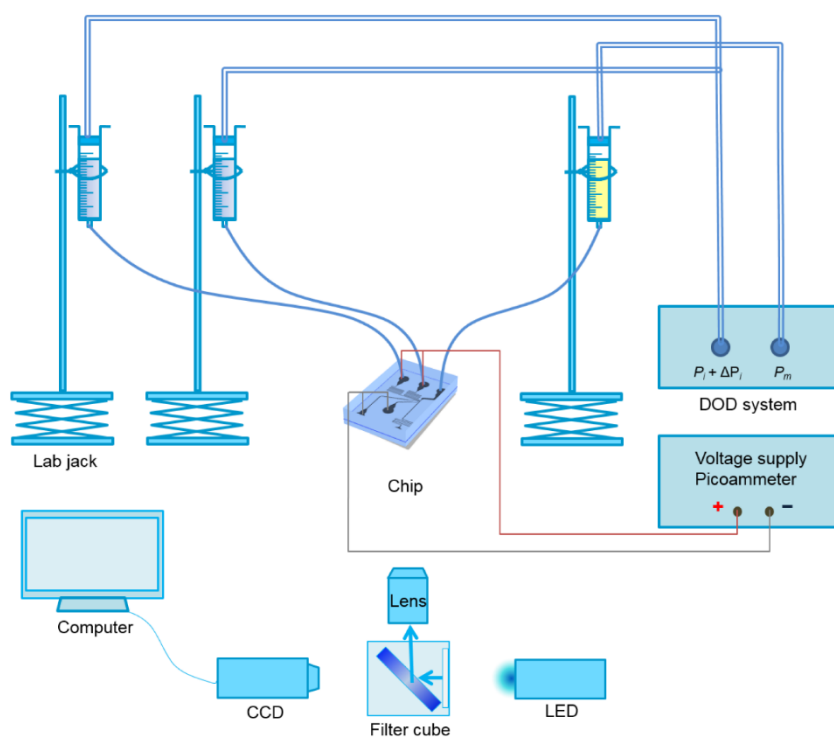


Figure S2. A schematic diagram showing the experimental setup including the lab jacks for pressure control, DOD system for droplet generation, imaging equipment and voltage supply.

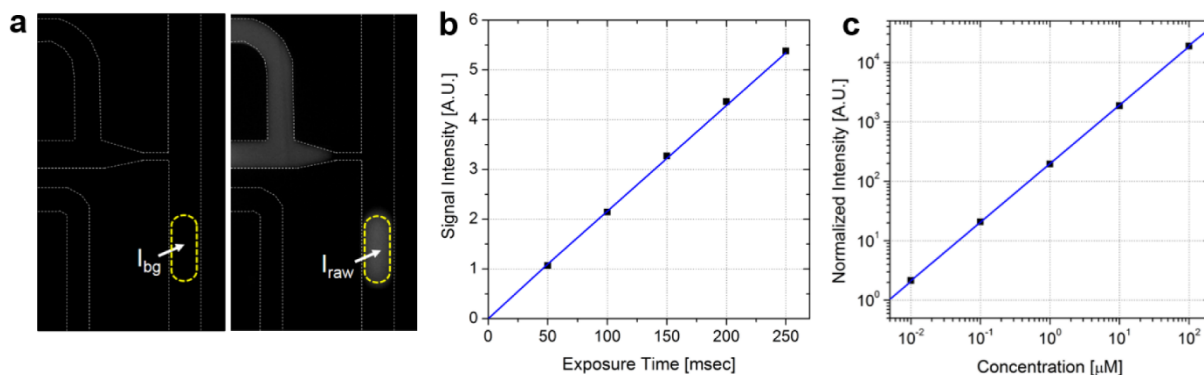


Figure S3. Calibration of fluorescence intensity for various sample concentrations and exposure times. (a) Images for measuring the background and raw intensity. (b) Background-subtracted intensity versus CCD exposure time for 100 nM FITC-BSA. (c) Normalized intensity versus concentration of FITC-BSA.